Cell Host & Microbe
Article

HIV-1 Nef Interferes with Host Cell Motility by Deregulation of Cofilin

Bettina Stolp,[1] Michal Reichman-Fried,[4] Libin Abraham,[1,2] Xiaoyu Pan,[1] Simone I. Giese,[1] Sebastian Hannemann,[1] Polyxeni Goulimari,[3] Erez Raz,[4] Robert Grosse,[3] and Oliver T. Fackler[1,*]
[1]Department of Virology, Im Neuenheimer Feld 324
[2]The Hartmut Hoffmann-Berling International Graduate School of Molecular and Cellular Biology, Im Neuenheimer Feld 282
[3]Institute of Pharmacology, Im Neuenheimer Feld 366
University of Heidelberg, 69120 Heidelberg, Germany
[4]Institute for Cell Biology, University of Münster, 48149 Münster, Germany
*Correspondence: oliver.fackler@med.uni-heidelberg.de
DOI 10.1016/j.chom.2009.06.004

SUMMARY

HIV-1 Nef is a key factor in AIDS pathogenesis. Here, we report that Nef potently inhibits motility of fibroblasts and chemotaxis of HIV-1-infected primary human T lymphocytes toward the chemokines SDF-1α, CCL-19, and CCL-21 ex vivo. Furthermore, Nef inhibits guided motility of zebrafish primordial germ cells toward endogenous SDF-1a in vivo. These migration defects result from Nef-mediated inhibition of the actin remodeling normally triggered by migratory stimuli. Nef strongly induces phosphorylation of cofilin, inactivating this evolutionarily conserved actin-depolymerizing factor that promotes cell motility when unphosphorylated. Nef-dependent cofilin deregulation requires association of Nef with the cellular kinase Pak2. Disruption of Nef-Pak2 association restores the cofilin phosphorylation levels and actin remodeling that facilitate cell motility. We conclude that HIV-1 Nef alters Pak2 function, which directly or indirectly inactivates cofilin, thereby restricting migration of infected T lymphocytes as part of a strategy to optimize immune evasion and HIV-1 replication.

INTRODUCTION

The host cell cytoskeleton plays a key role in the life cycle of viral pathogens whose propagation depends on mandatory intracellular steps. Viruses have consequently evolved strategies to modulate actin as well as microtubule filament systems to facilitate cell entry, intracellular transport, and egress of new viral progeny. Such strategies were also adopted by human retroviruses, such as the human immunodeficiency virus type 1 (HIV-1), that rely on actin remodeling for early entry and postentry steps during productive infection (Bukrinskaya et al., 1998; Jiménez-Baranda et al., 2007; McDonald et al., 2002; Yoder et al., 2008). Which cytoskeleton machineries are specifically targeted and by which mechanism HIV-1 affects host cell cytoskeleton remodeling, however, have remained unclear.

Remodeling of the cytoskeleton is also essential for directed movement of host cells themselves (Fackler and Grosse, 2008; Pollard and Borisy, 2003). While individual cell types exhibit motility in response to different exogenous triggers and use distinct types of cell movement depending on their physiological environment, core principles of cell motility probably apply to most scenarios (Rafelski and Theriot, 2004). One central aspect of directed cell motility is polarization of the moving cell, including translocation of the microtubule organizing center (MTOC) and the Golgi apparatus toward the direction of cell movement (Nabi, 1999). Also, the actin cytoskeleton undergoes dynamic changes in response to a migratory stimulus, typically leading to pronounced actin polymerization and depolymerization events that critically determine a cell's motile capacity. Such actin remodeling is subject to tight control, primarily by de novo nucleation of actin filaments (Chhabra and Higgs, 2007). In addition, F-actin disassembly via depolymerization factors such as cofilin also contributes to actin remodeling by providing F-actin fragments as substrate for new filaments (Bamburg and Bernstein, 2008).

The Nef protein of HIV-1 is a 25–35 kDa myristoylated protein that is expressed abundantly already at early stages of HIV-1 infection. Importantly, Nef expression is a prerequisite for efficient HIV-1 replication in the infected host. The absence of Nef, therefore, significantly slows down or completely abolishes development of acquired immunodeficiency syndrome (AIDS) (Deacon et al., 1995; Kestler et al., 1991). Moreover, isolated Nef expression in transgenic mice is sufficient to establish AIDS-like depletion of $CD4^+$ T lymphocytes (Hanna et al., 1998). While these results clearly established Nef as a critical viral factor in AIDS pathogenesis, the molecular basis for this activity still remains unclear. Nef is a versatile manipulator of host cell vesicular transport and signal transduction processes, effects that are mediated by a plethora of protein interactions with host cell factors such as components of the endocytic sorting and T cell receptor (TCR) signaling machineries (Malim and Emerman, 2008). Many of these interactions were mapped to defined protein interaction surfaces of Nef. However, which of the proposed ligands are functionally relevant remains elusive (Geyer et al., 2001). While effects of Nef in receptor transport are relatively well defined (Roeth and Collins, 2006), Nef's effects on signal transduction are not well understood. In T lymphocytes, one of the main target cell populations of HIV, Nef predominantly affects signal transduction via the TCR. While Nef generally elevates the basal state of T cell activation, multiple effects of HIV-1 Nef in response to TCR engagement leading to

selective activation or inhibition, respectively, of distinct downstream signaling events have been observed (Haller et al., 2006; Iafrate et al., 1997; Schindler et al., 2006; Schrager and Marsh, 1999). By the combination of these effects, Nef may prevent premature activation-induced death of infected cells while simultaneously increasing their permissivity for HIV-1 replication (Fackler et al., 2007). In addition, Nef prevents T lymphocyte chemotaxis toward the chemoattractant SDF-1α (Choe et al., 2002), but the mechanism and in vivo relevance of this activity are unclear.

Several protein assemblies have been described to interact with select surfaces on Nef and mediate individual downstream effects on T lymphocyte homeostasis. These include the kinase complex NAK-C, which facilitates transcription of the viral genome (Witte et al., 2004) and association of Nef with DOCK2-ELMO1, a complex implied in Nef's effect on T lymphocyte chemotaxis (Janardhan et al., 2004). In addition, Nef associates with a highly active population of the cellular kinase Pak2 in the context of a labile multiprotein complex (Nunn and Marsh, 1996; Rauch et al., 2008; Renkema et al., 1999). Pak2 is a member of the group I family of p21-activated kinases that act as downstream effectors of the activated Rho GTPases Cdc42 and Rac1 to modulate various processes such as cytoskeletal organization, transcription, and cell survival (Bokoch, 2003). In line with these functions of Pak2, Nef was suggested to modulate such cellular processes via its association with Pak2 (Haller et al., 2006; Lu et al., 1996; Wolf et al., 2001), but without establishing a direct role of Pak2 in these effects or addressing their mechanism or physiological relevance. To address these issues, we analyze here the effects of HIV-1 Nef on host cell motility. The results of these analyses unravel that the pathogenicity factor, via its Pak2 association, prevents actin remodeling to impair host cell motility in vitro and in vivo and define deregulation of cofilin as an underlying mechanism.

RESULTS

Inhibition of Fibroblast Wound Closure by Nef

To address whether Nef generally affects cell migration, we expressed the HIV protein in the hamster fibroblast cell line CHO, a cell type that supports key biological activities of Nef (Keppler et al., 2005). Stable cell lines were generated that express a control GFP or a GFP fusion protein of wild-type (WT) HIV-1_{SF2} Nef, a functional homolog of nonfusion Nef, in a doxycycline (Dox)-inducible manner. Cells were grown to confluence, and cell motility was analyzed after scratch wounding of the monolayer (Figure 1). GFP-expressing control cells rapidly migrated into the scratch wound, resulting in wound closure approximately after 15–20 hr (Figures 1A and 1B, Movie S1). In contrast, expression of WT Nef in the two independent CHO clones analyzed (WT12, used in all subsequent experiments, and WT17) caused a marked reduction in cell migration, resulting in incomplete wound closure even after 24 hr (Figures 1A and 1B, Movie S2). Kinetic analysis of the wound width over time identified the 20 hr postwounding time point as a robust parameter to quantify differences between GFP- and Nef-expressing cells (Figures 1B and 1C) and revealed a more than 8-fold reduction in motility of Nef-expressing cells as compared to control cells. This deficit was specific for the expression of Nef, as cells in which Nef expression had not been induced (−Dox) displayed normal wound healing.

To map the molecular determinants of Nef that are responsible for the inhibition of wound closure, various inducible cell lines were generated for the expression of Nef mutants. Dox concentrations were titrated by flow cytometry to result in levels of Nef.GFP expression that in all cell clones were comparable or higher than for WT Nef.GFP (Figures S1A and S1B). All mutant Nef proteins displayed the expected subcellular localization (intracellular membranes, plasma membrane, and cytoplasm), and Nef expression had no impact on cell proliferation (Figures S1C and S1D). The LLAA Nef variant (leucine 168 and 169 mutated to alanine to disrupt Nef's interaction with the clathrin endocytosis machinery) interfered with wound healing as efficiently as WT Nef (Figures 1D and S2). In contrast, several Nef mutants were impaired in inhibiting wound-healing motility even when expressed at higher levels than WT Nef: G2A (a nonmyristoylated Nef with reduced membrane association), E4A4 (glutamic acid 66–69 mutated to alanine to disrupt association with the PACS sorting adaptor), and AxxA (proline 76 and 79 mutated to alanine to disrupt interaction with SH3 domain-containing ligands). In contrast to these mutants that are deficient in several biological properties of Nef, a single point mutation, F195A/I, which specifically interrupts the association of Nef with the cellular kinase Pak2 without affecting other Nef activities (O'Neill et al., 2006; Rauch et al., 2008), even more potently abrogated the Nef-mediated inhibition of cell motility 20 hr after wounding. Kinetic analysis revealed that Nef F195A-expressing cells exhibit an initial motility defect after scratch wounding, but then accelerate to result in wound closure indistinguishable from GFP-expressing control cells (Figure S2F).

Nef Affects Actin Turnover in Migrating Cells

To determine the mechanism by which Nef interferes with wound healing, cell polarization and cytoskeletal organization was compared in GFP- and WT Nef.GFP-expressing CHO cells. While WT Nef-expressing cells displayed a slight defect in polarization of the Golgi apparatus toward the wound (Figures S3A and S3B), analysis of Nef mutants ruled out that this phenomenon is required for the migration defect of Nef-expressing cells (data not shown). Polarization of the MTOC toward the wound was unaffected by Nef expression (Figures S3C and S3D), and organization of total as well as detyrosinated, stable microtubules, which are required for wound healing (Cook et al., 1998), was normal in the presence of Nef (Figures S3E and S3F). In contrast, analysis of F-actin organization revealed pronounced effects of Nef expression. While all cells displayed low levels of F-actin directly after wounding (t = 0 hr), GFP-expressing control cells showed pronounced filament assembly after 4 hr (Figures 1E and S4A). This induction of actin filaments was fully inhibited in the presence of WT Nef that, in turn, induced the formation of small punctuate F-actin aggregates in the cytoplasm instead. While Nef mutants LLAA or G2A, E4A4, and AxxA showed WT or intermediate activity in blocking filament assembly, respectively, Nef F195A was entirely deficient and allowed for pronounced formation of actin filaments (Figures 1F and S4A). Across this panel of CHO cell lines, we observed a strong correlation between inhibition of wound closure and filament assembly by Nef (Figure S4B). Since the pivotal role of

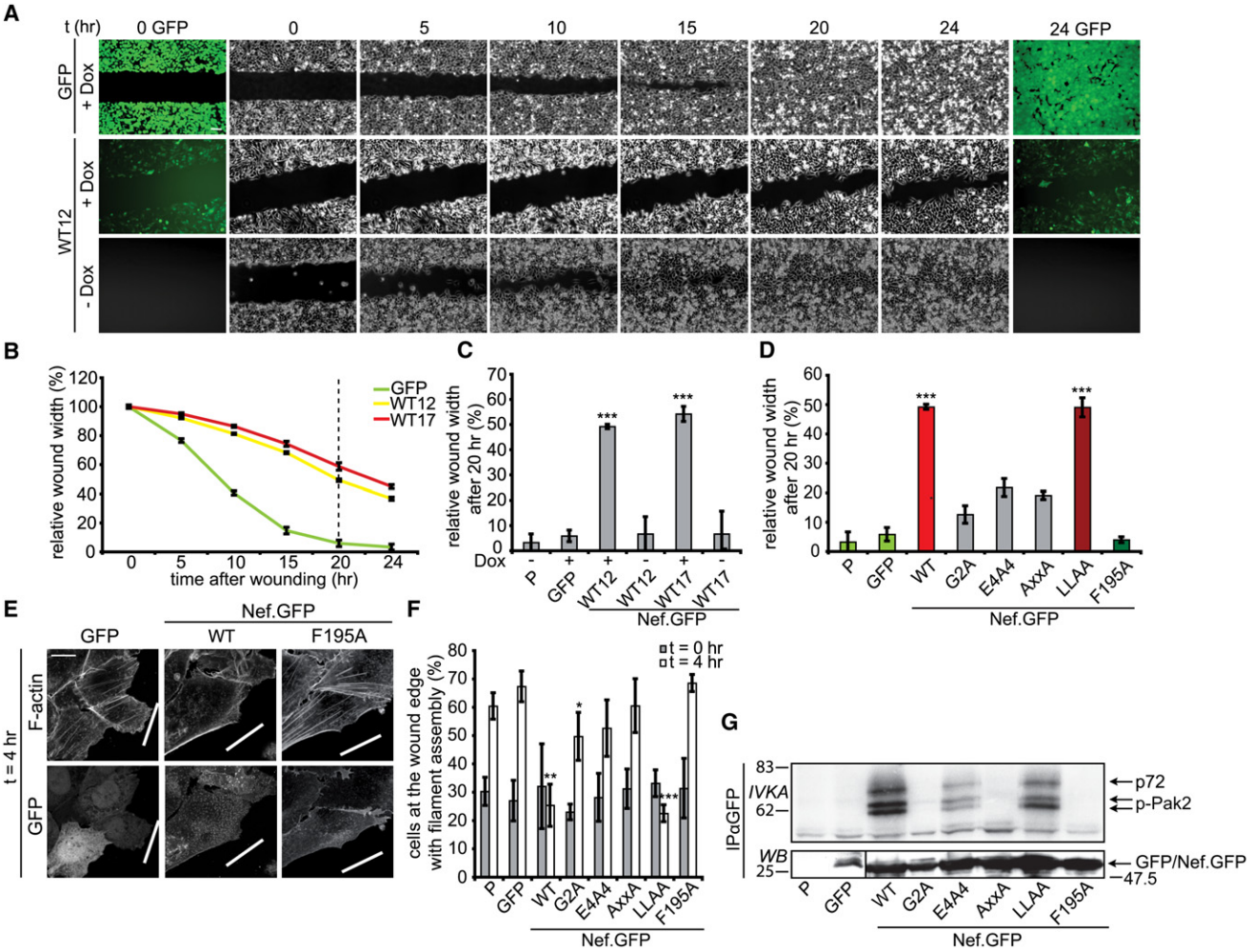

Figure 1. HIV-1 Nef Interferes with Wound Healing Cell Motility and Wound-Induced Actin Filament Assembly

(A) Representative micrographs of wound closure kinetics of the indicated cell lines. CHO cells stably transduced with expression constructs for GFP or WT Nef.GFP were induced for transgene expression (+Dox) or left untreated (−Dox) and grown to confluency. After introduction of a wound by a pipette tip, cell migration into the wound was monitored over 24 hr. Scale bar = 100 μm.

(B) Wound closure time course of GFP-expressing CHO cells versus the WT Nef.GFP-expressing CHO clones 12 and 17. Depicted are mean values ± SEM of 7–9 independent experiments.

(C and D) Quantification of relative wound width at 20 hr after wounding of the indicated cell clones (P, parental) as indicated by the dotted line in (B). Shown is the mean ± SEM of 3–9 independent experiments. P values are calculated relative to the GFP control.

(E) Representative confocal micrographs of the indicated CHO cell clones at the wound edge 4 hr after wounding. Cells were fixed and stained with phalloidin to reveal F-actin. Bold white lines indicate the trajectory of the wound. Scale bar = 10 μm. Pictures of additional Nef mutants and cells directly after wounding are shown in Figure S4A.

(F) Quantification of actin filament assembly. Shown are mean values ± SD from three independent experiments of cells displaying actin stress fibers near the wound, with at least 100 cells counted per experiment.

(G) Nef-associated Pak2 activity. CHO cells expressing the indicated GFP/Nef.GFP proteins were transfected with a Pak2 expression construct and subjected to anti-GFP immunoprecipitation and subsequent in vitro kinase assay (IVKA). Phosphorylated endogenous and overexpressed Pak2 (p-PAK2) or immunoisolated GFP/Nef.GFP present in the IVKA were detected by autoradiography and western blotting, respectively (IVKA and WB panels). p72 designates an unidentified Pak2 substrate.

the F195 residue for Nef-Pak2 association has thus far only been investigated in human cells, we next tested whether this mutation also disrupts the interaction in CHO cells. In vitro kinase analysis (IVKA) of immunoisolated Nef indeed revealed the specific association of WT, but not G2A, AxxA, and F195A Nef with autophosphorylated Pak2 (Figure 1G), indicating that Pak2 association might be involved in the Nef-mediated inhibition of actin remodeling and wound closure.

Nef Prevents SDF-1α-Induced T Lymphocyte Membrane Ruffling and Chemotaxis

We next asked whether Nef also interferes with actin remodeling and cell motility in natural target cells of HIV-1 infection such as T lymphocytes. Chemotaxis was used as an experimental system, since incubation of T lymphocytes with chemoattractants such as SDF-1α results in pronounced actin remodeling that is required for directional movement toward chemokine gradients

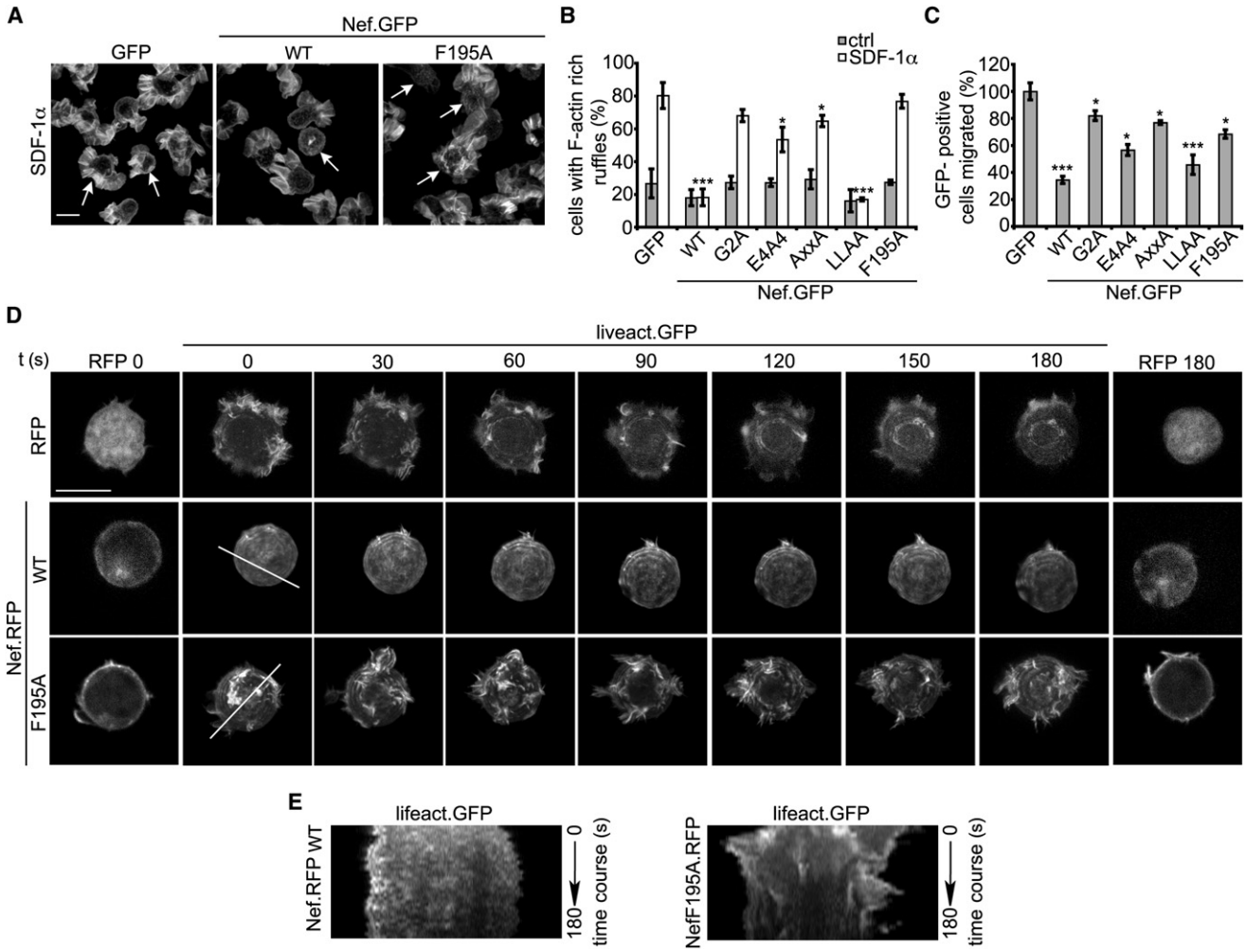

Figure 2. Nef Inhibits SDF-1α-Induced Actin Ruffling and Chemotaxis in T Lymphocytes

(A) Representative maximum projections of confocal Z stacks of Jurkat T lymphocytes (Jurkat TAg) transiently expressing the indicated GFP fusion proteins. Cells were fixed 20 min after treatment with 200 ng/ml SDF-1α and stained for F-actin. Arrows indicate transfected cells; GFP signals and additional Nef mutants are shown in Figure S4D. Scale bar = 10 μm.

(B) Frequency of the cells shown in (A) and Figure S4D that display membrane ruffling in response to treatment with SDF-1α or a solvent control (ctrl). Depicted are mean values from four independent experiments ± SD with at least 100 cells analyzed per condition. P values are calculated relative to the GFP control.

(C) Chemotaxis toward SDF-1α. Jurkat T lymphocytes (Jurkat E6-1) expressing the indicated proteins were subjected to a transwell chemotaxis assay. Depicted is the percentage of GFP-positive cells that migrated toward 10 ng/ml SDF-1α over 2 hr. Values are the mean with SEM from four experiments performed in triplicates. P values are calculated relative to the GFP control.

(D) Still images of the time-lapse Movies S3, S4, and S5. Jurkat T lymphocytes (Jurkat-CCR7) were cotransfected with RFP, WT, or F195A Nef.RFP and lifeact.GFP to reveal F-actin. Shown are maximum intensity projections of the GFP signal every 30 s. The first and the last panel show single confocal pictures of the RFP signal before and after acquisition of the movie.

(E) Kymographs from the white lines of the cells shown in (D).

(Nishita et al., 2005). Transient expression of WT Nef in Jurkat T lymphocytes caused a marked inhibition of SDF-1α-induced actin rearrangement and membrane ruffling (see Figures 2A and S4D for analysis of fixed cells). The activity pattern of Nef mutants correlated well with the previous results in CHO cells, with the F195 residue being one essential determinant for this phenotype (Figure 2B). This was particularly apparent in real-time confocal analysis, which revealed dynamic protrusion and retraction of actin-rich lamellododia and filopodia in the presence of RFP or Nef F195A.RFP, while WT Nef.RFP-expressing cells failed to undergo such dynamic plasma membrane reorganization (Figures 2D and 2E, Movies S3, S4, and S5). Moreover, Nef caused a marked reduction of T lymphocyte chemotaxis toward SDF-1α (Figure 2C) (Choe et al., 2002). This inhibition in T lymphocyte chemotaxis was significantly impaired, but not entirely abrogated for the Nef F195A mutant. WT and F195A Nef proteins both induced comparable, moderate downregulation of the SDF-1α receptor CXCR4 from the cell surface (Schindler et al., 2007 and data not shown) and associated to a similar extent with DOCK2-ELMO1 (Figure S5). Inhibition of SDF-1α-induced membrane ruffling and chemotaxis was observed, albeit with varying efficiency, with different *nef* alleles from HIV-1, HIV-2,

and simian immunodeficiency virus (SIV), demonstrating that they represent conserved activities of lentiviral Nef proteins (Figures S6A–S6C). Notably, a strong correlation was observed between the ability of Nef variants and mutants to interfere with SDF-1α-induced membrane ruffling and chemotaxis (Figures S4C and S6D). To extend these findings to the context of HIV-1 infection, primary human peripheral blood lymphocytes (PBLs) were infected with HIV-1 WT, HIV-1ΔNef lacking Nef expression, or an isogenic virus expressing the F195I Nef mutant and analyzed for their ability to undergo membrane ruffling and chemotaxis upon treatment with the CXCR4 ligand SDF-1α or the CCR7 ligands CCL-19 or CCL-21, respectively (Figure 3). Infection with WT, but not ΔNef HIV-1, potently blocked the formation of large polarized membrane ruffles in the presence of any of the three chemokines and impaired lymphocyte chemotaxis (Figures 3A–3C and S7A, Movies S6 and S7). These Nef effects depended again on F195 and Nef effects on T lymphocyte chemotaxis and membrane ruffling correlated with each other.

Effects of Nef on SDF-1a-Mediated Zebrafish Primordial Germ Cell Migration In Vivo

We sought to explore whether Nef can also affect migration of cells in the context of an intact organism at physiological SDF-1α concentrations. The lack of an HIV-1-permissive small animal and limited transduction rates of primary mouse T lymphocytes prevented us from performing such experiments in mice in the context of HIV-1 infection or upon adoptive transfer of Nef-expressing T lymphocytes. To address functions of Nef in vivo, we studied primordial germ cell (PGC) migration in zebrafish embryos. Migration of the CXCR4b-expressing PGCs toward cells expressing SDF-1a, a zebrafish ortholog of mammalian SDF-1α, represents a well-established model for an SDF-1-guided migration process that typically culminates in clustering of PGCs at the site of gonad development in 24 hr old zebrafish embryos (Doitsidou et al., 2002) (Figure 4A, left panel). When PGCs expressed WT Nef.GFP, arrival of these cells at the target site in 24 hr old embryos was dramatically disrupted, such that 91% of the embryos showed PGCs to be distributed in ectopic positions throughout the embryo (average of 62% ectopic PGCs in 106 embryos) (Figure 4A). This severe migration phenotype was virtually reversed upon expression of the Nef mutant F195A protein fused to GFP: In the majority (80%, n = 48) of these embryos, PGCs arrived at the target site in a manner indistinguishable from that observed in control embryos (Figure 4A). To analyze the basis for the compromised ability of WT Nef-expressing PGCs to reach the target, cells expressing either WT or F195A Nef were monitored by time-lapse microscopy, and their tracks of migration were delineated. Similar to normal PGCs (Reichman-Fried et al., 2004), F195A-expressing cells displayed long and directional tracks (Figures 4B and 4C, Movie S8). Tracks of WT Nef-expressing PGCs, however, were significantly shorter and coiled, reflecting severe inhibition of motility (Figures 4B and 4C, Movie S9). Furthermore, direct examination of the frequency of motile cells in each experimental group revealed that while 75% of the F195A-expressing cells were motile and exhibited normal directed migration (211 cells analyzed in 16 embryos), the majority of cells expressing WT Nef (77%) were nonmotile and largely remained on the spot when compared to somatic cells (160 cells analyzed in 12 embryos) (Figure 4D, Movies S8 and S9). Together, expression of WT Nef potently inhibits PGC motility in vivo in a manner that is dependent on F195, the site that enables its association with Pak2.

Nef Inactivates Cofilin by Inducing Its Hyperphosphorylation via Association with Pak2 Activity

To address whether the association of Nef with Pak2 is instrumental for the inhibition of actin remodeling and cell motility by the viral protein, we tested if signaling events downstream of Pak2 were altered in the presence of Nef. Indeed, cofilin, a key regulator of actin depolymerization that is inactivated by phosphorylation of serine at position 3 downstream of p21-activated kinases Pak1 and Pak2 (Edwards et al., 1999; Misra et al., 2005), was markedly hyperphosphorylated in the presence of WT Nef in CHO cells directly or 4 hr after wounding (Figure 5A). In most experiments, a reduction in levels of phosphorylated cofilin (p-cofilin) 4 hr postwounding was observed in GFP control cells. In contrast, WT Nef-expressing cells never displayed a similar reduction in cofilin phosphorylation after scratch wounding. Phosphorylation of Src and Merlin was unaffected by Nef expression. Similar to the results obtained for cell migration and actin remodeling, the F195 residue and the PxxP motif of Nef were essential for cofilin phosphorylation (Figures 5B and 5C). Cofilin hyperphosphorylation in Nef-expressing cells was sustained for at least 24 hr after scratch wounding (Figure 5D). In contrast to the Pak effector cofilin, GTPase activity of the Rac1 and Cdc42 upstream regulators of Pak activity was unaffected in cells expressing WT or F195A Nef (Figure 5E). In addition to Pak-dependent pathways, cofilin phosphorylation can also be regulated via the Rho-ROCK pathway (Maekawa et al., 1999). Inhibition of ROCK activity by the specific inhibitor Y27632, however, did not reverse Nef-induced hyperphosphorylation of cofilin (Figure 5F). Cofilin inactivation was also observed in Jurkat T lymphocytes expressing WT Nef.GFP or HIV-1-infected PBLs (Figures 6A–6E, S7B, and S7C). Quantification on a single-cell level revealed that, even in the absence of any stimulation, significantly more Nef-expressing cells displayed elevated p-cofilin levels in comparison to the controls (Figures 6B and 6E). Based on pixel quantifications of confocal Z stacks of individual cells, Nef expression caused a more than 4-fold increase in levels of p-cofilin per cell (Figure 6C). To test the contribution of Pak2 to Nef's effects on cofilin deregulation directly, we used RNAi-mediated knockdown of Pak2 expression to analyze the role of the kinase for Nef's inhibitory effects in Jurkat T lymphocytes (Figures 6F–6I and S7D). We previously established that potent reduction of Pak2 protein levels in these cells causes a marked, but incomplete, decrease in Nef-associated Pak2 activity, by 35% (Rauch et al., 2008). Basal p-cofilin levels were not affected by Pak2 RNAi in the absence of Nef. In contrast, Pak2 knockdown significantly reduced the frequency and magnitude of cofilin hyperphosphorylation in the presence of Nef (see also Figure S8F). We conclude that Nef induces the accumulation of phosphorylated, inactive cofilin and that Pak2 is critical for this deregulation of cofilin.

Nef-Associated Pak2 Determines Inhibition of Cell Motility by Nef, Possibly by Direct Phosphorylation of Cofilin

We next determined the role of Pak2 for the effects of Nef on actin remodeling and cell motility. Analysis of F-actin

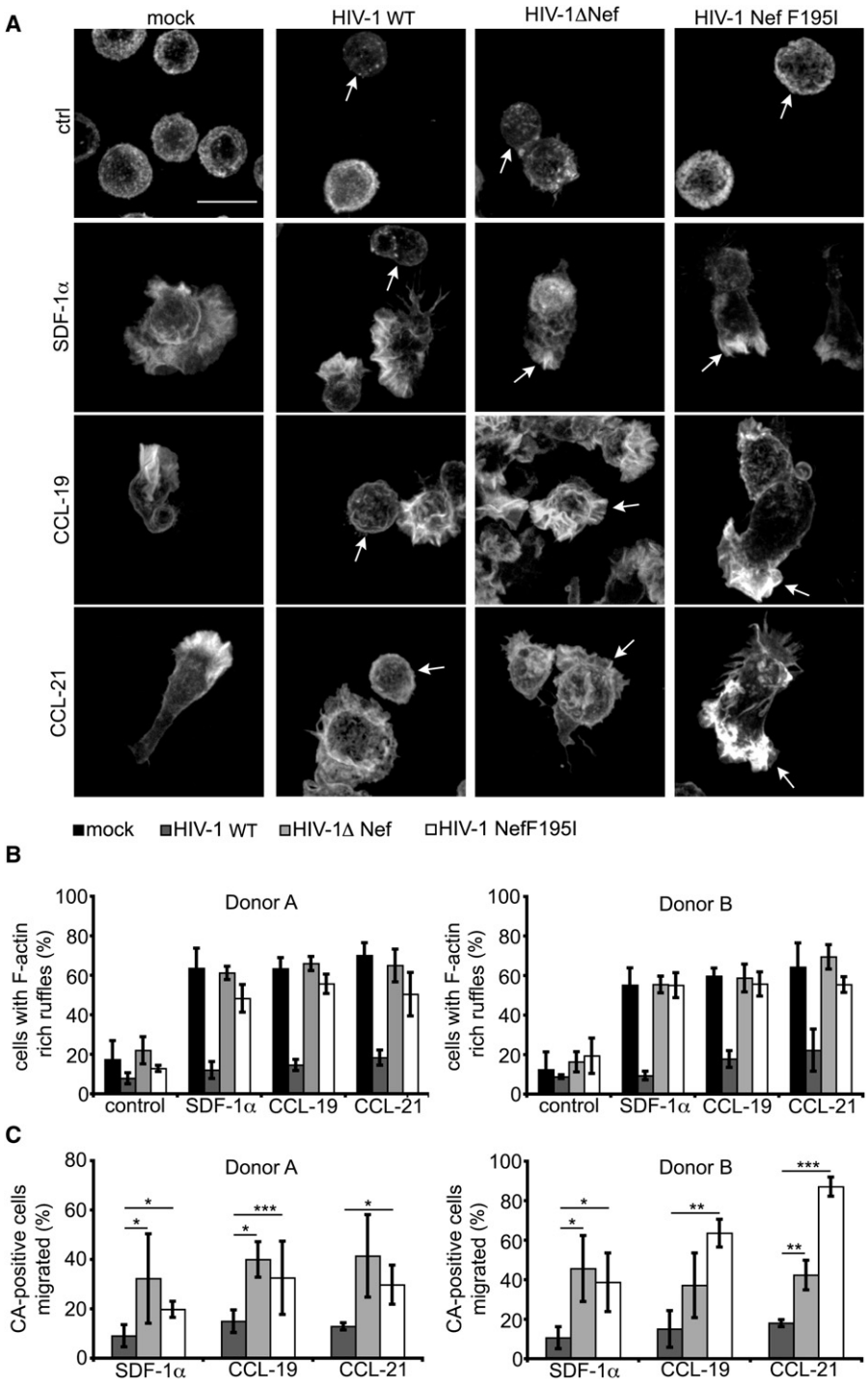

Figure 3. Nef Inhibits Chemokine-Induced Actin Remodeling and Chemotaxis in HIV-1-Infected Primary Human T Lymphocytes

(A) Representative maximum projections of confocal Z stacks of PBLs infected with WT HIV-1 (HIV-1 WT), its *nef*-deleted counterpart HIV-1ΔNef, or the isogenic virus HIV-1 Nef F195I. Cells were treated with 200 ng/ml SDF-1α, CCL-19, or CCL-21 for 20 min or left untreated (ctrl); fixed; and stained for intracellular p24CA and F-actin. Arrows indicate infected cells; p24CA signals are shown in Figure S7A. Scale bar = 10 μm.

(B) Frequency of the cells shown in (A) with membrane ruffling. Depicted are mean values from quadruplicate infections ± SD for two independent donors with at least 100 cells analyzed per condition.

(C) Chemotaxis toward SDF-1α, CCL-19, or CCL-21 of two independent donors. PBLs infected with the indicated viruses were subjected to a transwell chemotaxis assay. Depicted is the percentage of p24CA-positive cells that migrated toward 10 ng/ml SDF-1α or 25 ng/ml CCL-19 or CCL-21 over 2 hr. Values are the mean with SD from triplicate infections.

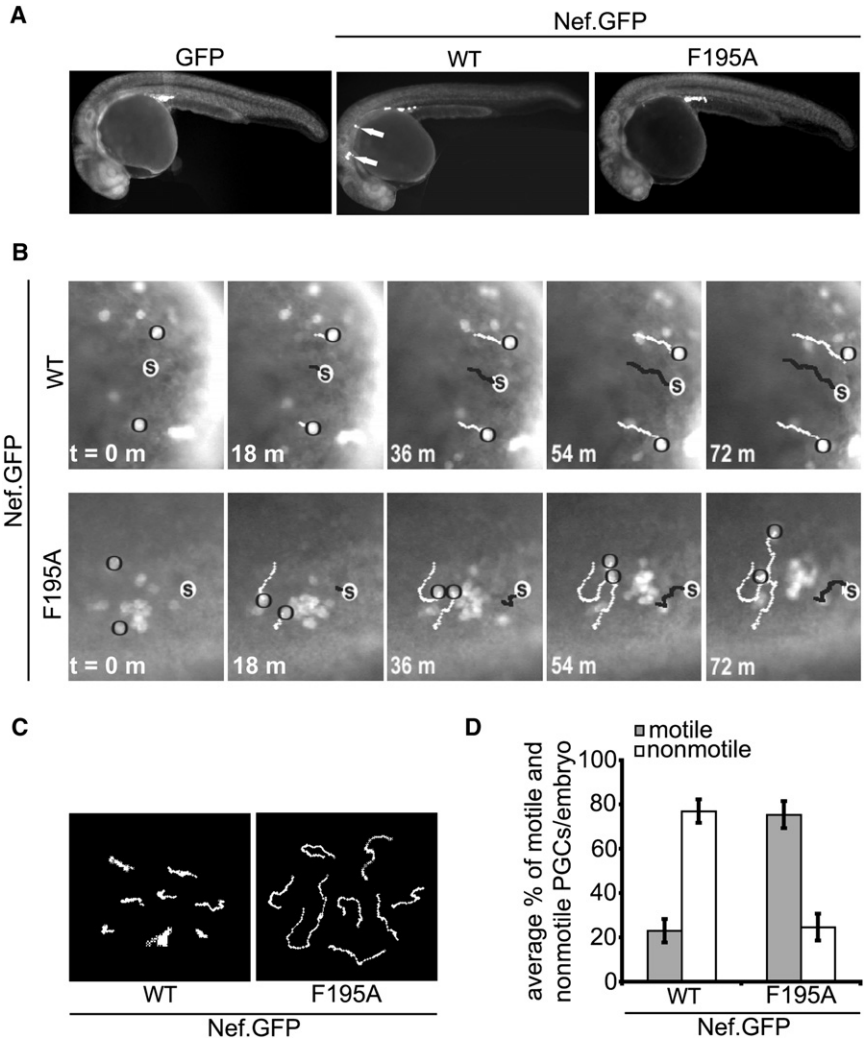

Figure 4. Nef Inhibits Motility of Zebrafish PGCs

(A) Images of representative zebrafish embryos, at 24 hr after fertilization, whose PGCs express GFP alone (left panel) or GFP fusion of either WT Nef (middle panel) or F195A Nef mutant (right panel). White arrows point at PGCs found at abnormal (ectopic) positions.

(B) Snapshots from the time-lapse Movies S8 and S9. The migration of PGCs expressing F195A or WT Nef.GFP was followed for 72 min. PGCs (circled in black) are tracked as indicated by the white line in comparison to a black track generated by a moving somatic cell (whitened cell marked with an "s").

(C) Examples for 72 min migration tracks of PGCs expressing F195A or WT Nef.GFP as indicated in (B). The migration of PGCs was followed in time-lapse movies and subtracted for somatic cell movement. Short tracks reflect inhibition of motility and are the basis for the inability of many PGCs to reach their target at 24 hr of development.

(D) Average frequency of motile and nonmotile PGCs expressing F195A or WT Nef.GFP. The results are presented as average percentage of motile and nonmotile PGCs per embryo. Error bars represent SEM of at least 80 cells in eight embryos.

reorganization revealed that treatment of cells with control or Pak2-specific RNAi had no effect on cell morphology prior to stimulation with SDF-1α and did not affect membrane ruffle formation of GFP-expressing cells in response to the chemokine (Figures 7A, 7B, and S7E). Thus, Pak2 does not control actin remodeling, chemotaxis, and cofilin phosphorylation in our cells in the absence of Nef. In turn, knockdown of Pak2 markedly diminished Nef's ability to block actin remodeling. This rescue was partial, but correlated well with the 35% reduction in Nef-associated Pak2 activity observed under these conditions. Consistently, expression of a dominant-negative Pak significantly enhanced SDF-1α-mediated membrane ruffling in the presence of Nef (Figure S9). Pak2 knockdown also significantly improved the migratory response of Nef-expressing cells toward SDF-1α, however less efficiently than in the actin remodeling assay (Figure 7D). Similarly in CHO fibroblasts, Pak2 RNAi almost completely rescued Nef-mediated disruption of actin filament assembly without appreciable effects in the absence of Nef and partially released the block of wound closure and cofilin hyperphosphorylation imposed by the viral protein (Figure S8). In an attempt to define the mechanism by which Nef-associated Pak2 targets cofilin, we failed to overcome the Nef-dependent inhibition of actin ruffle formation and cofilin deregulation in T lymphocytes by coexpression of dominant-negative variants of kinases (LIMK, TESK) or phosphatases (slingshot, chronophin) with known roles in cofilin regulation (Edwards et al., 1999; Huang et al., 2006; Misra et al., 2005; data not shown). This prompted us to test whether Pak2 might phosphorylate cofilin directly. Indeed, recombinant Pak2 was able to phosphorylate cofilin in vitro, a reaction that was not affected by the presence of Nef (Figures 7E and 7F). Importantly, cofilin also served as efficient substrate of Nef-Pak2 complexes isolated from T lymphocytes with WT, but not F195A Nef (Figure 7G). While these results do not exclude the involvement of other components of the Nef-Pak2 complex, they suggest that Nef-associated Pak2 itself mediates phosphorylation of cofilin. Nef may thus impair actin remodeling and directional cell motility by hijacking Pak2 via a physical association that retargets the biological activity of the kinase toward direct phosphorylation of cofilin.

DISCUSSION

This study reveals that the HIV-1 pathogenicity factor Nef interferes with cell motility by blocking chemoattractant-triggered actin remodeling. The effect of Nef on cell motility occurs independently of the cellular context ex vivo in Nef-expressing fibroblasts and HIV-1-infected primary T lymphocytes, as well as in zebrafish PGCs in vivo, and represents a conserved activity of

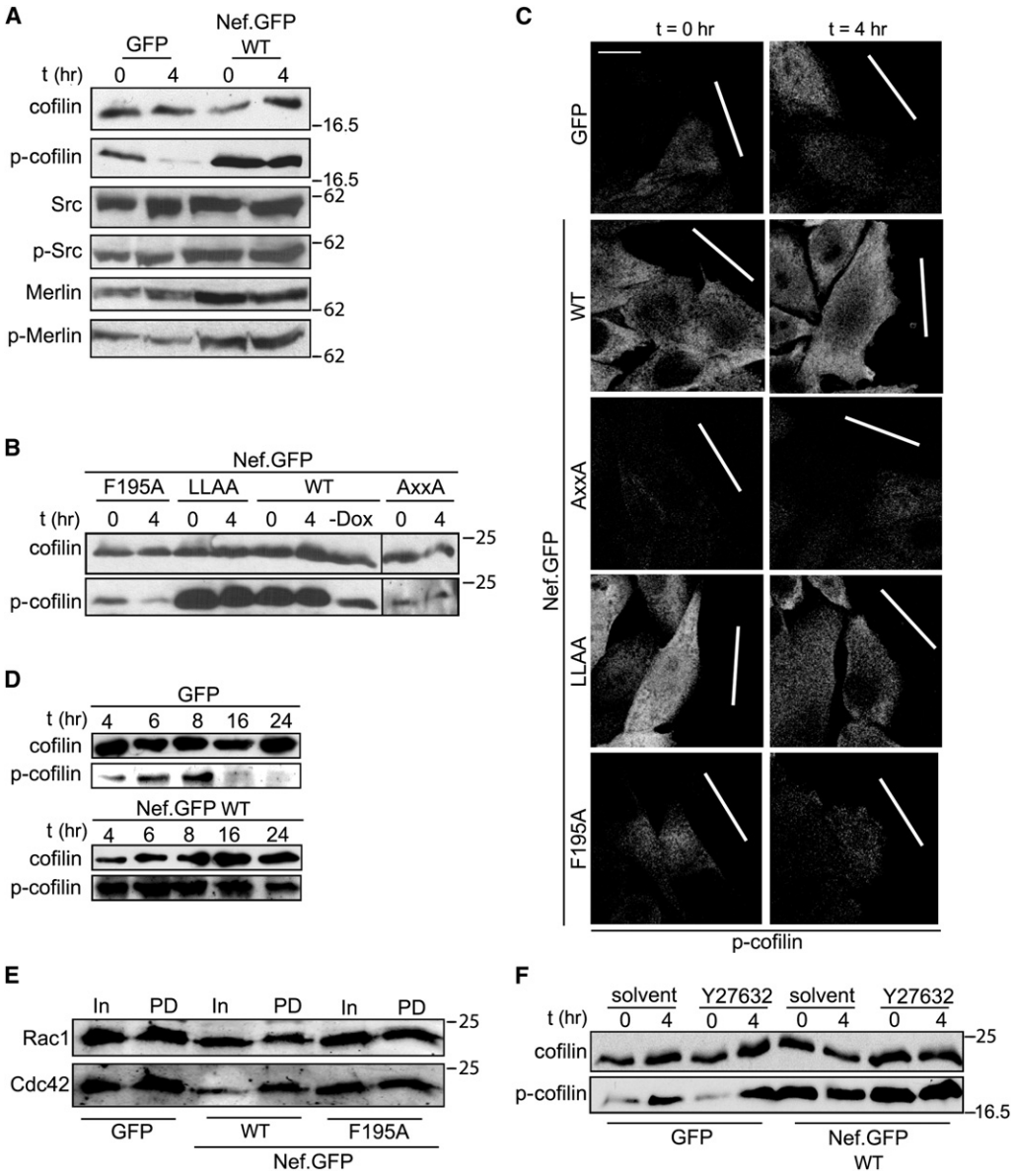

Figure 5. Nef Induces Cofilin Hyperphosphorylation

(A–D) Multiple wounds were introduced to confluent CHO cells expressing GFP or WT Nef.GFP (A and D) or the indicated Nef mutants (B). Cells were harvested at the indicated time points after wounding and analyzed by western blotting using the indicated antibodies. −Dox indicates that expression of Nef has not been induced. Note that quantification of the merlin/p-merlin ratio (A) from five independent experiments did not reveal statistically significant differences between GFP and Nef.GFP-expressing cells and that in (D), 3× more protein was loaded per lane for GFP than for Nef.GFP-expressing cells in order to detect a p-cofilin signal. Representative confocal micrographs of the cells analyzed in (A) and (B) following staining for p-cofilin are shown in (C). Bold white lines indicate the trajectory of the wound. Scale bar = 10 μm.

(E) Rac1 and Cdc42 activity levels of CHO cells expressing the indicated proteins determined by western blotting following pulldown by the GST-CRIB peptide of Pak1 (In, input; PD, pulldown).

(F) Levels of p-cofilin in CHO cells expressing GFP or WT Nef.GFP in the absence or presence of ROCK inhibitor Y27632.

Nef proteins from various HIV-1, HIV-2, and SIV strains. Mechanistic analyses demonstrate that inhibition of actin remodeling is mediated by Nef via its ability to associate with the cellular kinase Pak2, resulting in hyperphosphorylation and thereby inactivation of the evolutionary conserved actin depolymerization factor, cofilin. This is achieved by retargeting Pak2 toward cofilin, which can serve as direct Pak2 substrate in the presence of Nef. HIV, thus, has evolved the viral factor Nef to hijack the host cell cytoskeleton for impairment of cell motility.

While alterations in actin organization in the presence of Nef were reported from several cell systems (Campbell et al., 2004; Haller et al., 2006; Lu et al., 2008; Quaranta et al., 2003), mechanism and functional consequence of this phenomenon have remained largely unclear. Addressing these issues by the

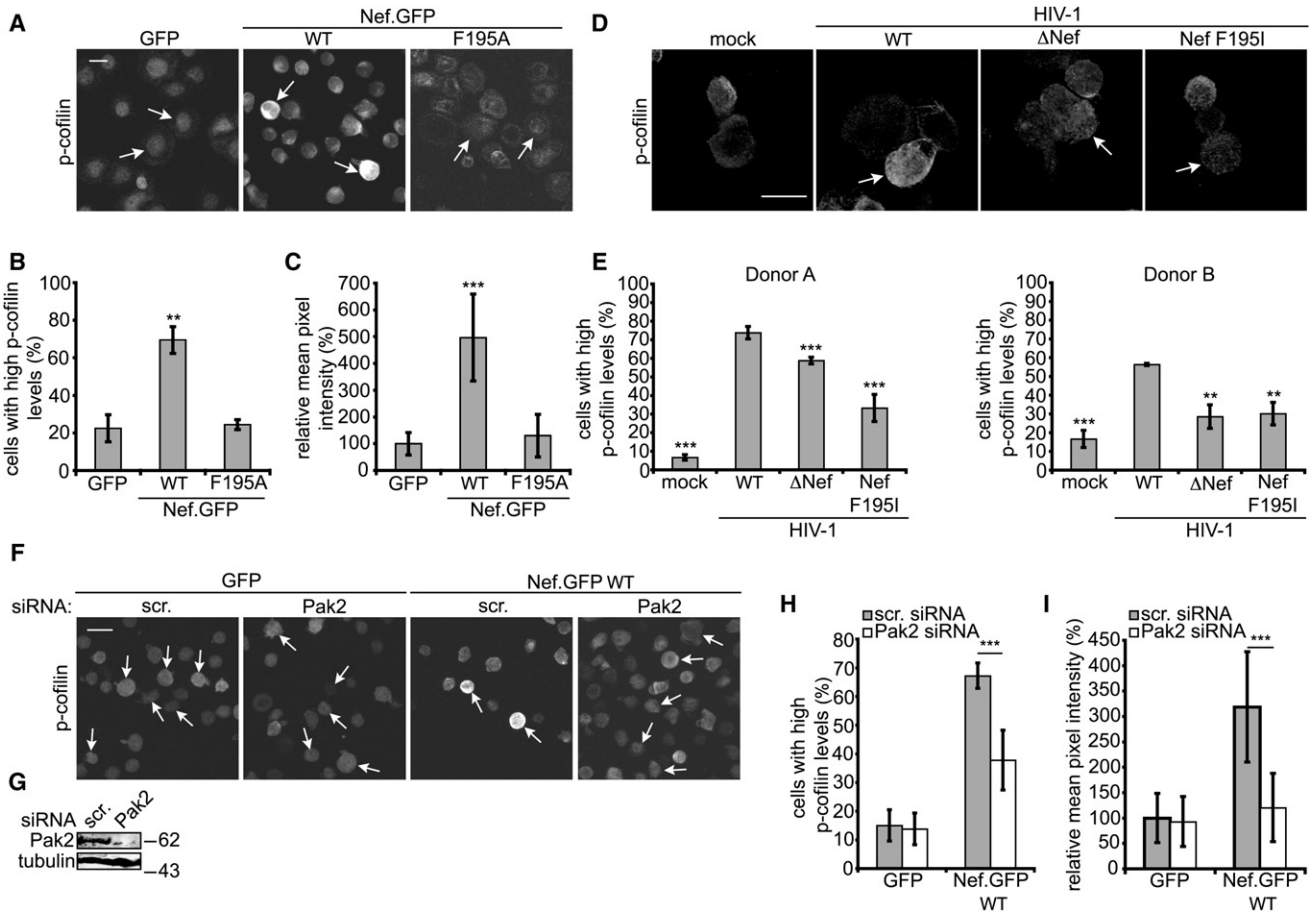

Figure 6. Nef-Induced Cofilin Hyperphosphorylation in Infected Primary Human T Lymphocytes Depends on Pak2

(A) Representative sum-intensity projections of confocal Z stacks of Jurkat T lymphocytes (Jurkat TAg) transiently expressing the indicated GFP fusion proteins. Cells were plated onto cover glasses, fixed, and stained for p-cofilin. Arrows indicate transfected cells; the GFP signal is shown in Figure S7B. Scale bar = 10 μm.

(B) Frequency of the cells shown in (A) with high p-cofilin levels. Depicted are mean values ± SD from three independent experiments with at least 100 cells analyzed per transfection, with cells scored as containing high p-cofilin levels when they were apparently brighter than untransfected neighboring cells. P values are calculated relative to the GFP-transfected cells.

(C) Relative mean pixel intensity of the cells in (A). Depicted are mean values ± SD from at least ten representative cells. P values are calculated relative to the GFP-transfected cells.

(D) P-cofilin levels in PBLs infected with HIV-1 WT, HIV-1ΔNef, or HIV-1 Nef F195I. Cells were analyzed as in (A) with an additional stain for p24CA (shown in Figure S7C). Arrows indicated infected cells. Scale bar = 10 μm.

(E) Frequency of the cells shown in (D) with high p-cofilin levels. Depicted are mean values ± SD from quadruplicate infections of two independent donors with at least 100 cells analyzed per infection. P values are calculated relative to the WT HIV-1-infected cells.

(F) P-cofilin levels of Jurkat T lymphocytes (Jurkat TAg) transiently transfected with siRNA oligos specific for Pak2 or a nonspecific scrambled siRNA (scr.) together with an expression plasmid for GFP or Nef.GFP. Arrows indicate transfected cells; the GFP signal is shown in Figure S7D. Scale bar = 10 μm.

(G) Western blot analysis of the cells used in (F).

(H) Frequency of the cells shown in (F) with high p-cofilin levels. Depicted are mean values ± SD from three independent experiments with at least 100 cells analyzed per transfection.

(I) Relative mean pixel intensities of the cells in (F). Depicted are mean values ± SD from at least ten representative cells per condition.

use of Nef mutants and Pak2-specific RNAi revealed, first, that the association of Nef with Pak2 activity is essential for the interference with chemoattractant-induced actin remodeling. Second, we identify cofilin as a downstream target of the Nef-Pak2 complex that causes a marked and sustained enrichment of the phosphorylated, inactive form of cofilin, even prior to migratory stimulation. Third, cofilin deregulation was demonstrated to be directly involved in Nef-mediated inhibition of actin remodeling and cell motility. This identification of cofilin as a target for the regulation of cell motility is consistent with cofilin's well-characterized role as master switch of actin remodeling in motile cells. Severing of actin filaments by active cofilin results in depolymerization of F-actin and generation of F-actin fragments that serve as substrate for nucleation of new filaments (Bamburg and Bernstein, 2008). This activity is essential for the directionality of cell movement during, e.g., lymphocyte chemotaxis or tumor cell invasion (Nishita et al., 2005; Wang et al., 2007). Cofilin is tightly regulated in migrating cells by phosphorylation of serine at position 3. It is therefore conceivable that Nef-induced inactivation of cofilin results in a net reduction of

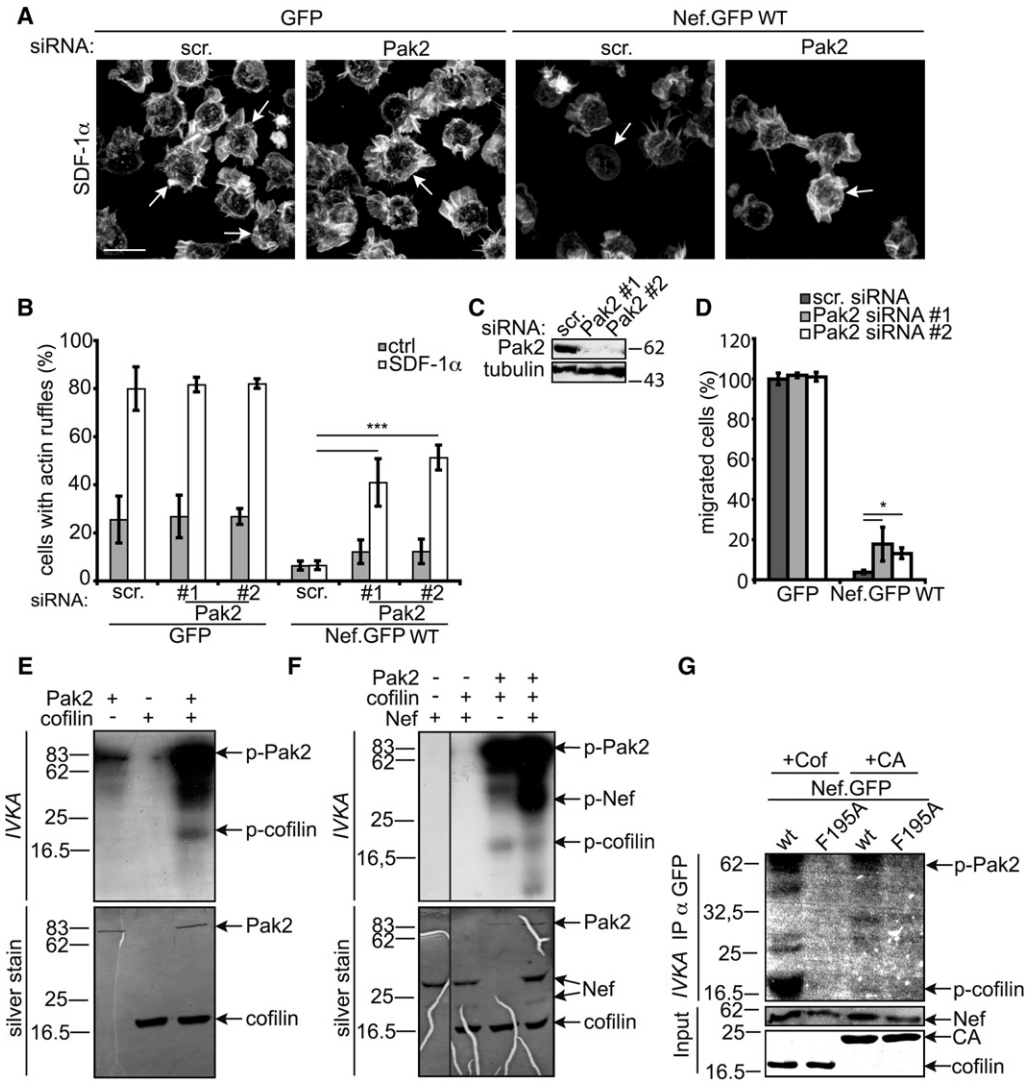

Figure 7. Nef-Associated Pak2 Is Involved in the Interference of Nef with Ruffle Formation and Chemotaxis in T Lymphocytes and Phosphorylates Cofilin

(A) Membrane ruffling analysis as in Figure 2A of Jurkat T lymphocytes (Jurkat CCR7) transfected with siRNA oligos specific for Pak2 or a nonspecific scrambled siRNA (scr.) together with an expression plasmid for GFP or WT Nef.GFP. Arrows indicate transfected cells; the GFP signal is shown in Figure S7E. Scale bar = 10 μm.

(B) Frequency of the cells shown in (A) that display membrane ruffling. Depicted is the mean ± SD of 3–8 independent experiments with at least 100 cells analyzed per condition.

(C) Western blot analysis of lysates of the cells used in (A).

(D) Chemotaxis toward SDF-1α. Cells shown in (A) were subjected to a transwell chemotaxis assay. Depicted is the percentage of GFP-positive cells that migrated toward 10 ng/ml SDF-1α over 2 hr. Values are the mean with SEM from four experiments performed in triplicates.

(E) Pak2 phosphorylates cofilin in vitro. Recombinant GST-Pak2 and cofilin were subjected to an in vitro kinase assay (IVKA), separated by SDS-PAGE, and analyzed by silver stain and autoradiography.

(F) Experiment as in (E) in the presence of recombinant myristoylated Nef. Pak2 phosphorylates cofilin in vitro in the presence of Nef.

(G) Nef-associated Pak2 phosphorylates cofilin. Jurkat TAg cells expressing WT or F195A Nef.GFP were subjected to anti-GFP immunoprecipitation and subsequent in vitro kinase assay (IVKA) in the presence of recombinant cofilin or HIV-1 CA as substrate. Phosphorylated Pak2 (p-PAK2) and p-cofilin present in the IVKA were detected by autoradiography. Nef in the input was detected by western blot; recombinant cofilin and p24CA by Coomassie stain.

actin turnover and subsequent cell motility. Interestingly, cofilin was also identified recently as regulator of HIV-1 entry (Yoder et al., 2008) and thus emerges as an important player in HIV-1's host cell interactions.

However, rescue of cofilin deregulation in Nef-expressing cells by Pak2-specific RNAi improved but did not fully restore their motility. This reflects, at least in part, the presence of residual Nef-Pak2 association in the RNAi experiments due to incomplete knockdown of Pak2 expression (Rauch et al., 2008), but may also indicate the involvement of additional cytoskeleton regulation downstream of Nef-Pak2. However, the Nef F195A mutant, which lacks any detectable Pak2 kinase association and cofilin

deregulation, maintained some inhibitory activity despite normal actin remodeling. Thus, Nef likely exerts effects on cell motility via a second, actin-independent mechanism. With DOCK2-ELMO1 and Lck, Nef functionally interacts with at least two additional host cell factors implicated in cell motility control (Fukui et al., 2001; Janardhan et al., 2004; Okabe et al., 2005; Thoulouze et al., 2006). While both factors appear dispensable for effects on actin via Nef-Pak2 (Rauch et al., 2008) (Figures S5 and S10), their intrinsic requirement for cell motility precludes direct analysis of their contribution to cell motility restriction by Nef. In addition, Nef disturbs a variety of intracellular sorting processes (Roeth and Collins, 2006) and might affect cell motility via such mechanisms.

The results of this study provide important insight into the mechanism of cofilin deregulation by Nef. Notably, reduction of Pak2 expression had no major effects on actin remodeling, cofilin phosphorylation, and cell motility in the absence of Nef. Endogenous Pak2 therefore does not control these parameters in our cell systems. Our results are thus most consistent with a scenario in which Nef subverts intrinsic properties of Pak2. This might have included alterations in known pathways that govern cofilin phosphorylation; however, we failed to detect a role of such factors for Nef action (data not shown). Instead, we discovered that cofilin can be phosphorylated in the presence of Nef-Pak2 complexes, suggesting that the association with the viral protein alters the substrate specificities of Pak2 to retarget its activity toward cofilin. Consistent with such a scenario, the subcellular localization of phosphorylated Pak was altered by the presence of Nef in motile cells (Figure S11). The presence of another cofilin kinase in the Nef-associated protein complex, however, cannot be excluded. Efforts to unravel the molecular details of the retargeting mechanism, including attempts to determine the full composition of the labile and short-lived Nef-Pak2 complex, are currently ongoing.

We consider the introduction of zebrafish PGC migration as an experimental system for in vivo studies on Nef function to be an important aspect of this work. Zebrafish are readily accessible to specific expression of genes in germ cells and real-time imaging analyses. These features allowed us to quantify, in a physiological context, cell motility events analogous to T lymphocyte chemotaxis that are, upon transient expression of genes of interest, exceedingly difficult to assess in other in vivo experimental systems. Although limited to processes that are conserved between the natural target cells of a given pathogen and zebrafish germ cells, zebrafish PGC migration is likely to further serve as a useful model for the functional analysis of pathogen-host interactions in the case of HIV-1, but also other viral pathogens, such as Epstein-Barr virus (Ehlin-Henriksson et al., 2006) or human T lymphotropic virus type I (Arai et al., 1998).

For HIV-1 Nef, the high degree of evolutionary conservation of the mechanism by which HIV-1 hijacks an endogenous cellular pathway to affect host cell actin remodeling and motility implies that this provides the virus with significant benefits in the infected host. In newly infected individuals, HIV-1-loaded dendritic cells transport virus from mucosal surfaces to lymph nodes, where virus is efficiently transmitted to T lymphocytes (Wu and KewalRamani, 2006). Subsequent intra-lymph node motility of productively infected T lymphocytes ensures mounting of an appropriate humoral immune response by providing B lymphocyte stimulation, induction of germinal centers for specialized production of high-affinity antibodies, and surveillance of overall architecture and de novo genesis of lymph nodes as well as tertiary lymphatic tissue (Friedl and Weigelin, 2008; Stein and Nombela-Arrieta, 2005). Lymph node homing and intra-lymph node motility of T lymphocytes rely on sensing of chemokine gradients and chemotaxis toward SDF-1α, CCL-19, and CCL-21 (Wei et al., 2003). Thus, our results predict that Nef interferes with such motile events in infected individuals. Intriguingly, B lymphocyte dysfunction as consequence of disruption of germinal center formation is increasingly recognized as an important parameter in the symptom-complex AIDS (De Milito, 2004; Moir et al., 2008), a phenotype that is readily reflected in Nef-transgenic mice (Poudrier et al., 2001). Moreover, histological analysis of lymph nodes from macaques 2 weeks after infection with WT or ΔNef SIV detected ΔNef SIV-infected cells in germinal centers that were dramatically enlarged due to infiltration of infected cells. In stark contrast, WT SIV-infected cells were predominantly located in the paracortex, and B cell follicle displayed a normal architecture (Sugimoto et al., 2003). Together with the in vivo analyses presented here, these findings strongly suggest that Nef, by interfering with membrane ruffling and thus chemotaxis, prevents intra-lymph node migration of HIV-1/SIV-infected T lymphocytes to undermine the humoral immune response to virus infection. Simultaneously, reduced motility of HIV-1-infected T lymphocytes may result in the generation of microenvironments that are particularly prone to virus transmission to uninfected cells. Modulation of cell motility may thus emerge as an unexpected strategy to optimize immune evasion and replication of HIV-1 in the infected host.

EXPERIMENTAL PROCEDURES

Lymphocyte Ruffling and Chemotaxis Assay

Jurkat T lymphocytes (1×10^7) were electroporated (30–60 μg of plasmid DNA; 960 μF for Jurkat TAg, 850 μF for Jurkat E6-1 and Jurkat CCR7, 250 V, Biorad Genepulser; Munich) with GFP or Nef.GFP expression plasmids. For microscopy, cover glasses were incubated for 30 min at 37°C with 0.01% poly-L-lysine, washed two times with water, and kept in PBS at 4°C until usage. Twenty-four hours after transfection, cells were seeded onto treated cover glasses for 5 min at 37°C and either fixed directly for staining of p-cofilin or incubated with 200 ng/ml SDF-1α or solvent control for another 20 min at 37°C for the analysis of membrane ruffling before fixation. Chemotaxis assays were performed with three independent transfections per experiment. Twenty-four hours after transfection, cells were starved in medium containing 0.5% FCS and incubated for another 24 hr. Transwell inserts (5 μm pores, 24-well plates, Costar3421, Corning; Kaiserslautern, Germany) were equilibrated overnight. The bottom chamber of the transwell was filled with 450 μl starving medium containing 10 ng/ml or no SDF-1α; 1×10^6 transfected cells resuspended in 100 μl starving medium were loaded to the upper side of each transwell. Total cell numbers and transfection efficiencies were determined from another 100 μl aliquot of the identical cell suspension. Cells were allowed to chemotax for 2 hr at 37°C before cells in the lower chamber were collected and analyzed by FACS (FACScalibur, BD; Heidelberg, Germany) for 1 min monitoring GFP-expressing cells. In the absence of a stimulus, 1%–5% of the input cells migrated into the lower chamber of the transwell, whereas in the presence of SDF-1α, typically 30%–60% of the cells chemotaxed. Percentage of GFP-positive cells migrated relative to transfection efficiency was calculated to address inhibitory effects.

Expression and Analysis of WT and F195A Nef in PGCs of Zebrafish Embryos

Directing expression of various genes specifically to PGCs is facilitated by fusing the gene of interest to the 3′ untranslated region of *nanos*-1 (*nos*3′UTR), a zebrafish germ cell-specific gene (Köprunner et al., 2001). Capped sense RNA of WT or F195A *nef* fused to *gfp* and to *nos*3′UTR or of *gfp* alone fused to *nos*3′UTR was synthesized with the MessageMachine kit (Ambion; Darmstadt, Germany) and microinjected into zebrafish embryos (450 pg per embryo) at one-cell stage. Fish used are of the AB background. Epifluorescence images of 24 hr embryos were captured with a 5× objective using the Axioplan2 microscope (Zeiss; Göttingen, Germany) controlled by MetaMorph software (Universal Imaging; Sunnyvale, CA). Time-lapse movies for track and motility analysis were generated with a 10× objective. Frames were captured at 1 min intervals, and for tracking of migrating germ cells, the "Track Objects" software module of MetaMorph was used. Tracks delineating active migration of PGCs were corrected for movement originating in the surrounding cells that passively drag PGCs along. For better visualization of PGCs in this analysis, *gfp- nos*3′UTR RNA was injected (150 pg per embryo) along with WT or F195A *nef* RNA.

Statistical Evaluation

Statistical significance was calculated by performing a Student's t test (***, $p < 0.0005$; **, $p < 0.005$; *, $p < 0.05$).

SUPPLEMENTAL DATA

Supplemental Data include Supplemental Experimental Procedures, Supplemental References, 12 figures, and nine movies and can be found online at http://www.cell.com/cell-host-microbe/supplemental/S1931-3128(09)00216-9.

ACKNOWLEDGMENTS

We are grateful to Walter Nickel, Scott R. Struthers, Michael Sixt, Vanda Bartonova, Hans-Georg Kräusslich, Matthias Geyer, and Felix Wieland for the kind gift of reagents; to Oliver Keppler for critical comments on the manuscript; to the FACS sorting facility of SFB638 and the Nikon Imaging Center (EXC81) for service; and to Nadine Tibroni for expert technical help. This project was supported financially by the Deutsche Forschungsgemeinschaft (SFB638, project A11 to O.T.F., GRK1188 fellowships to B.S. and S.H., Cellular Networks PhD fellowship to L.A., and GR 2111/1-3 to R.G.) O.T.F. and R.G. are members of the CellNetworks Cluster of Excellence EXC81.

Received: February 12, 2009
Revised: April 30, 2009
Accepted: June 1, 2009
Published: August 19, 2009

REFERENCES

Arai, M., Ohashi, T., Tsukahara, T., Murakami, T., Hori, T., Uchiyama, T., Yamamoto, N., Kannagi, M., and Fujii, M. (1998). Human T-cell leukemia virus type 1 Tax protein induces the expression of lymphocyte chemoattractant SDF-1/PBSF. Virology *241*, 298–303.

Bamburg, J.R., and Bernstein, B.W. (2008). ADF/cofilin. Curr. Biol. *18*, R273–R275.

Bokoch, G.M. (2003). Biology of the p21-activated kinases. Annu. Rev. Biochem. *72*, 743–781.

Bukrinskaya, A., Brichacek, B., Mann, A., and Stevenson, M. (1998). Establishment of a functional human immunodeficiency virus type 1 (HIV-1) reverse transcription complex involves the cytoskeleton. J. Exp. Med. *188*, 2113–2125.

Campbell, E.M., Nunez, R., and Hope, T.J. (2004). Disruption of the actin cytoskeleton can complement the ability of Nef to enhance human immunodeficiency virus type 1 infectivity. J. Virol. *78*, 5745–5755.

Chhabra, E.S., and Higgs, H.N. (2007). The many faces of actin: matching assembly factors with cellular structures. Nat. Cell Biol. *9*, 1110–1121.

Choe, E.Y., Schoenberger, E.S., Groopman, J.E., and Park, I.W. (2002). HIV Nef inhibits T cell migration. J. Biol. Chem. *277*, 46079–46084.

Cook, T.A., Nagasaki, T., and Gundersen, G.G. (1998). Rho guanosine triphosphatase mediates the selective stabilization of microtubules induced by lysophosphatidic acid. J. Cell Biol. *141*, 175–185.

De Milito, A. (2004). B lymphocyte dysfunctions in HIV infection. Curr. HIV Res. *2*, 11–21.

Deacon, N.J., Tsykin, A., Solomon, A., Smith, K., Ludford-Menting, M., Hooker, D.J., McPhee, D.A., Greenway, A.L., Ellett, A., Chatfield, C., et al. (1995). Genomic structure of an attenuated quasi species of HIV-1 from a blood transfusion donor and recipients. Science *270*, 988–991.

Doitsidou, M., Reichman-Fried, M., Stebler, J., Köprunner, M., Dorries, J., Meyer, D., Esguerra, C.V., Leung, T., and Raz, E. (2002). Guidance of primordial germ cell migration by the chemokine SDF-1. Cell *111*, 647–659.

Edwards, D.C., Sanders, L.C., Bokoch, G.M., and Gill, G.N. (1999). Activation of LIM-kinase by Pak1 couples Rac/Cdc42 GTPase signalling to actin cytoskeletal dynamics. Nat. Cell Biol. *1*, 253–259.

Ehlin-Henriksson, B., Mowafi, F., Klein, G., and Nilsson, A. (2006). Epstein-Barr virus infection negatively impacts the CXCR4-dependent migration of tonsillar B cells. Immunology *117*, 379–385.

Fackler, O.T., and Grosse, R. (2008). Cell motility through plasma membrane blebbing. J. Cell Biol. *181*, 879–884.

Fackler, O.T., Alcover, A., and Schwartz, O. (2007). Modulation of the immunological synapse: a key to HIV-1 pathogenesis? Nat. Rev. Immunol. *7*, 310–317.

Friedl, P., and Weigelin, B. (2008). Interstitial leukocyte migration and immune function. Nat. Immunol. *9*, 960–969.

Fukui, Y., Hashimoto, O., Sanui, T., Oono, T., Koga, H., Abe, M., Inayoshi, A., Noda, M., Oike, M., Shirai, T., and Sasazuki, T. (2001). Haematopoietic cell-specific CDM family protein DOCK2 is essential for lymphocyte migration. Nature *412*, 826–831.

Geyer, M., Fackler, O.T., and Peterlin, B.M. (2001). Structure–function relationships in HIV-1 Nef. EMBO Rep. *2*, 580–585.

Haller, C., Rauch, S., Michel, N., Hannemann, S., Lehmann, M.J., Keppler, O.T., and Fackler, O.T. (2006). The HIV-1 pathogenicity factor Nef interferes with maturation of stimulatory T-lymphocyte contacts by modulation of N-Wasp activity. J. Biol. Chem. *281*, 19618–19630.

Hanna, Z., Kay, D.G., Rebai, N., Guimond, A., Jothy, S., and Jolicoeur, P. (1998). Nef harbors a major determinant of pathogenicity for an AIDS-like disease induced by HIV-1 in transgenic mice. Cell *95*, 163–175.

Huang, T.Y., DerMardirossian, C., and Bokoch, G.M. (2006). Cofilin phosphatases and regulation of actin dynamics. Curr. Opin. Cell Biol. *18*, 26–31.

Iafrate, A.J., Bronson, S., and Skowronski, J. (1997). Separable functions of Nef disrupt two aspects of T cell receptor machinery: CD4 expression and CD3 signaling. EMBO J. *16*, 673–684.

Janardhan, A., Swigut, T., Hill, B., Myers, M.P., and Skowronski, J. (2004). HIV-1 Nef binds the DOCK2-ELMO1 complex to activate rac and inhibit lymphocyte chemotaxis. PLoS Biol. *2*, E6.

Jiménez-Baranda, S., Gómez-Moutón, C., Rojas, A., Martínez-Prats, L., Mira, E., Ana Lacalle, R., Valencia, A., Dimitrov, D.S., Viola, A., Delgado, R., et al. (2007). Filamin-A regulates actin-dependent clustering of HIV receptors. Nat. Cell Biol. *9*, 838–846.

Keppler, O.T., Allespach, I., Schüller, L., Fenard, D., Greene, W.C., and Fackler, O.T. (2005). Rodent cells support key functions of the human immunodeficiency virus type 1 pathogenicity factor Nef. J. Virol. *79*, 1655–1665.

Kestler, H.W., 3rd, Ringler, D.J., Mori, K., Panicali, D.L., Sehgal, P.K., Daniel, M.D., and Desrosiers, R.C. (1991). Importance of the nef gene for maintenance of high virus loads and for development of AIDS. Cell *65*, 651–662.

Köprunner, M., Thisse, C., Thisse, B., and Raz, E. (2001). A zebrafish nanos-related gene is essential for the development of primordial germ cells. Genes Dev. *15*, 2877–2885.

Lu, T.C., He, J.C., Wang, Z.H., Feng, X., Fukumi-Tominaga, T., Chen, N., Xu, J., Iyengar, R., and Klotman, P.E. (2008). HIV-1 Nef disrupts the podocyte actin

cytoskeleton by interacting with diaphanous interacting protein. J. Biol. Chem. *283*, 8173–8182.

Lu, X., Wu, X., Plemenitas, A., Yu, H., Sawai, E.T., Abo, A., and Peterlin, B.M. (1996). CDC42 and Rac1 are implicated in the activation of the Nef-associated kinase and replication of HIV-1. Curr. Biol. *6*, 1677–1684.

Maekawa, M., Ishizaki, T., Boku, S., Watanabe, N., Fujita, A., Iwamatsu, A., Obinata, T., Ohashi, K., Mizuno, K., and Narumiya, S. (1999). Signaling from Rho to the actin cytoskeleton through protein kinases ROCK and LIM-kinase. Science *285*, 895–898.

Malim, M.H., and Emerman, M. (2008). HIV-1 accessory proteins–ensuring viral survival in a hostile environment. Cell Host Microbe *3*, 388–398.

McDonald, D., Vodicka, M.A., Lucero, G., Svitkina, T.M., Borisy, G.G., Emerman, M., and Hope, T.J. (2002). Visualization of the intracellular behavior of HIV in living cells. J. Cell Biol. *159*, 441–452.

Misra, U.K., Deedwania, R., and Pizzo, S.V. (2005). Binding of activated alpha2-macroglobulin to its cell surface receptor GRP78 in 1-LN prostate cancer cells regulates PAK-2-dependent activation of LIMK. J. Biol. Chem. *280*, 26278–26286.

Moir, S., Ho, J., Malaspina, A., Wang, W., DiPoto, A.C., O'Shea, M.A., Roby, G., Kottilil, S., Arthos, J., Proschan, M.A., et al. (2008). Evidence for HIV-associated B cell exhaustion in a dysfunctional memory B cell compartment in HIV-infected viremic individuals. J. Exp. Med. *205*, 1797–1805.

Nabi, I.R. (1999). The polarization of the motile cell. J. Cell Sci. *112*, 1803–1811.

Nishita, M., Tomizawa, C., Yamamoto, M., Horita, Y., Ohashi, K., and Mizuno, K. (2005). Spatial and temporal regulation of cofilin activity by LIM kinase and Slingshot is critical for directional cell migration. J. Cell Biol. *171*, 349–359.

Nunn, M.F., and Marsh, J.W. (1996). Human immunodeficiency virus type 1 Nef associates with a member of the p21-activated kinase family. J. Virol. *70*, 6157–6161.

O'Neill, E., Kuo, L.S., Krisko, J.F., Tomchick, D.R., Garcia, J.V., and Foster, J.L. (2006). Dynamic evolution of the human immunodeficiency virus type 1 pathogenic factor, Nef. J. Virol. *80*, 1311–1320.

Okabe, S., Fukuda, S., Kim, Y.J., Niki, M., Pelus, L.M., Ohyashiki, K., Pandolfi, P.P., and Broxmeyer, H.E. (2005). Stromal cell-derived factor-1alpha/CXCL12-induced chemotaxis of T cells involves activation of the RasGAP-associated docking protein p62Dok-1. Blood *105*, 474–480.

Pollard, T.D., and Borisy, G.G. (2003). Cellular motility driven by assembly and disassembly of actin filaments. Cell *112*, 453–465.

Poudrier, J., Weng, X., Kay, D.G., Paré, G., Calvo, E.L., Hanna, Z., Kosco-Vilbois, M.H., and Jolicoeur, P. (2001). The AIDS disease of CD4C/HIV transgenic mice shows impaired germinal centers and autoantibodies and develops in the absence of IFN-gamma and IL-6. Immunity *15*, 173–185.

Quaranta, M.G., Mattioli, B., Spadaro, F., Straface, E., Giordani, L., Ramoni, C., Malorni, W., and Viora, M. (2003). HIV-1 Nef triggers Vav-mediated signaling pathway leading to functional and morphological differentiation of dendritic cells. FASEB J. *17*, 2025–2036.

Rafelski, S.M., and Theriot, J.A. (2004). Crawling toward a unified model of cell mobility: spatial and temporal regulation of actin dynamics. Annu. Rev. Biochem. *73*, 209–239.

Rauch, S., Pulkkinen, K., Saksela, K., and Fackler, O.T. (2008). Human immunodeficiency virus type 1 Nef recruits the guanine exchange factor Vav1 via an unexpected interface into plasma membrane microdomains for association with p21-activated kinase 2 activity. J. Virol. *82*, 2918–2929.

Reichman-Fried, M., Minina, S., and Raz, E. (2004). Autonomous modes of behavior in primordial germ cell migration. Dev. Cell *6*, 589–596.

Renkema, G.H., Manninen, A., Mann, D.A., Harris, M., and Saksela, K. (1999). Identification of the Nef-associated kinase as p21-activated kinase 2. Curr. Biol. *9*, 1407–1410.

Roeth, J.F., and Collins, K.L. (2006). Human immunodeficiency virus type 1 Nef: adapting to intracellular trafficking pathways. Microbiol. Mol. Biol. Rev. *70*, 548–563.

Schindler, M., Münch, J., Kutsch, O., Li, H., Santiago, M.L., Bibollet-Ruche, F., Müller-Trutwin, M.C., Novembre, F.J., Peeters, M., Courgnaud, V., et al. (2006). Nef-mediated suppression of T cell activation was lost in a lentiviral lineage that gave rise to HIV-1. Cell *125*, 1055–1067.

Schindler, M., Rajan, D., Specht, A., Ritter, C., Pulkkinen, K., Saksela, K., and Kirchhoff, F. (2007). Association of Nef with p21-activated kinase 2 is dispensable for efficient human immunodeficiency virus type 1 replication and cytopathicity in ex vivo-infected human lymphoid tissue. J. Virol. *81*, 13005–13014.

Schrager, J.A., and Marsh, J.W. (1999). HIV-1 Nef increases T cell activation in a stimulus-dependent manner. Proc. Natl. Acad. Sci. USA *96*, 8167–8172.

Stein, J.V., and Nombela-Arrieta, C. (2005). Chemokine control of lymphocyte trafficking: a general overview. Immunology *116*, 1–12.

Sugimoto, C., Tadakuma, K., Otani, I., Moritoyo, T., Akari, H., Ono, F., Yoshikawa, Y., Sata, T., Izumo, S., and Mori, K. (2003). nef gene is required for robust productive infection by simian immunodeficiency virus of T-cell-rich paracortex in lymph nodes. J. Virol. *77*, 4169–4180.

Thoulouze, M.I., Sol-Foulon, N., Blanchet, F., Dautry-Varsat, A., Schwartz, O., and Alcover, A. (2006). Human immunodeficiency virus type-1 infection impairs the formation of the immunological synapse. Immunity *24*, 547–561.

Wang, W., Eddy, R., and Condeelis, J. (2007). The cofilin pathway in breast cancer invasion and metastasis. Nat. Rev. Cancer *7*, 429–440.

Wei, S.H., Parker, I., Miller, M.J., and Cahalan, M.D. (2003). A stochastic view of lymphocyte motility and trafficking within the lymph node. Immunol. Rev. *195*, 136–159.

Witte, V., Laffert, B., Rosorius, O., Lischka, P., Blume, K., Galler, G., Stilper, A., Willbold, D., D'Aloja, P., Sixt, M., et al. (2004). HIV-1 Nef mimics an integrin receptor signal that recruits the polycomb group protein Eed to the plasma membrane. Mol. Cell *13*, 179–190.

Wolf, D., Witte, V., Laffert, B., Blume, K., Stromer, E., Trapp, S., d'Aloja, P., Schürmann, A., and Baur, A.S. (2001). HIV-1 Nef associated PAK and PI3-kinases stimulate Akt-independent Bad-phosphorylation to induce anti-apoptotic signals. Nat. Med. *7*, 1217–1224.

Wu, L., and KewalRamani, V.N. (2006). Dendritic-cell interactions with HIV: infection and viral dissemination. Nat. Rev. Immunol. *6*, 859–868.

Yoder, A., Yu, D., Dong, L., Iyer, S.R., Xu, X., Kelly, J., Liu, J., Wang, W., Vorster, P.J., Agulto, L., et al. (2008). HIV envelope-CXCR4 signaling activates cofilin to overcome cortical actin restriction in resting CD4 T cells. Cell *134*, 782–792.